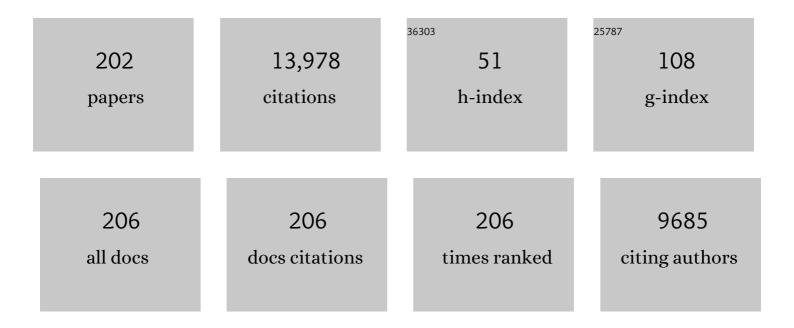
List of Publications by Year in descending order

Source: https://exaly.com/author-pdf/9513739/publications.pdf Version: 2024-02-01



SINA FADSILI

#	Article	IF	CITATIONS
1	Fast and Robust Multiframe Super Resolution. IEEE Transactions on Image Processing, 2004, 13, 1327-1344.	9.8	1,689
2	Kernel Regression for Image Processing and Reconstruction. IEEE Transactions on Image Processing, 2007, 16, 349-366.	9.8	1,114
3	Automatic segmentation of seven retinal layers in SDOCT images congruent with expert manual segmentation. Optics Express, 2010, 18, 19413.	3.4	639
4	Advances and challenges in super-resolution. International Journal of Imaging Systems and Technology, 2004, 14, 47-57.	4.1	526
5	Automatic segmentation of nine retinal layer boundaries in OCT images of non-exudative AMD patients using deep learning and graph search. Biomedical Optics Express, 2017, 8, 2732.	2.9	396
6	Fully automated detection of diabetic macular edema and dry age-related macular degeneration from optical coherence tomography images. Biomedical Optics Express, 2014, 5, 3568.	2.9	362
7	Quantitative Classification of Eyes with and without Intermediate Age-related Macular Degeneration Using Optical Coherence Tomography. Ophthalmology, 2014, 121, 162-172.	5.2	280
8	Kernel regression based segmentation of optical coherence tomography images with diabetic macular edema. Biomedical Optics Express, 2015, 6, 1172.	2.9	265
9	Multiframe demosaicing and super-resolution of color images. IEEE Transactions on Image Processing, 2006, 15, 141-159.	9.8	262
10	Photoreceptor Layer Thinning over Drusen in Eyes with Age-Related Macular Degeneration Imaged In Vivo with Spectral-Domain Optical Coherence Tomography. Ophthalmology, 2009, 116, 488-496.e2.	5.2	251
11	Sparsity based denoising of spectral domain optical coherence tomography images. Biomedical Optics Express, 2012, 3, 927.	2.9	225
12	Dry Age-Related Macular Degeneration: Mechanisms, Therapeutic Targets, and Imaging. , 2013, 54, ORSF68.		218
13	Progression of Intermediate Age-related Macular Degeneration with Proliferation and Inner Retinal Migration of Hyperreflective Foci. Ophthalmology, 2013, 120, 1038-1045.	5.2	208
14	Validated Automatic Segmentation of AMD Pathology Including Drusen and Geographic Atrophy in SD-OCT Images. , 2012, 53, 53.		204
15	Maturation of the Human Fovea: Correlation of Spectral-Domain Optical Coherence Tomography Findings With Histology. American Journal of Ophthalmology, 2012, 154, 779-789.e2.	3.3	193
16	Fast Acquisition and Reconstruction of Optical Coherence Tomography Images via Sparse Representation. IEEE Transactions on Medical Imaging, 2013, 32, 2034-2049.	8.9	191
17	Dynamics of Human Foveal Development after Premature Birth. Ophthalmology, 2011, 118, 2315-2325.	5.2	189
18	Anti-amyloid therapy protects against retinal pigmented epithelium damage and vision loss in a model of age-related macular degeneration. Proceedings of the National Academy of Sciences of the United States of America, 2011, 108, E279-87.	7.1	185

#	Article	IF	CITATIONS
19	Insights into Advanced Retinopathy of Prematurity Using Handheld Spectral Domain Optical Coherence Tomography Imaging. Ophthalmology, 2009, 116, 2448-2456.	5.2	165
20	INTRAOPERATIVE USE OF HANDHELD SPECTRAL DOMAIN OPTICAL COHERENCE TOMOGRAPHY IMAGING IN MACULAR SURGERY. Retina, 2009, 29, 1457-1468.	1.7	165
21	Integration of a Spectral Domain Optical Coherence Tomography System into a Surgical Microscope for Intraoperative Imaging. , 2011, 52, 3153.		165
22	Imaging the Infant Retina with a Hand-held Spectral-Domain Optical Coherence Tomography Device. American Journal of Ophthalmology, 2009, 147, 364-373.e2.	3.3	164
23	Deblurring Using Regularized Locally Adaptive Kernel Regression. IEEE Transactions on Image Processing, 2008, 17, 550-563.	9.8	143
24	Automated non-rigid registration and mosaicing for robust imaging of distinct retinal capillary beds using speckle variance optical coherence tomography. Biomedical Optics Express, 2013, 4, 803.	2.9	139
25	Retinal Artery-Vein Classification via Topology Estimation. IEEE Transactions on Medical Imaging, 2015, 34, 2518-2534.	8.9	126
26	Abnormal Foveal Morphology in Ocular Albinism Imaged With Spectral-Domain Optical Coherence Tomography. JAMA Ophthalmology, 2009, 127, 37.	2.4	124
27	Foveal avascular zone and foveal pit formation after preterm birth. British Journal of Ophthalmology, 2012, 96, 961-966.	3.9	110
28	Effect of Ciliary Neurotrophic Factor on Retinal Neurodegeneration in Patients with Macular Telangiectasia Type 2. Ophthalmology, 2019, 126, 540-549.	5.2	110
29	Segmentation Based Sparse Reconstruction of Optical Coherence Tomography Images. IEEE Transactions on Medical Imaging, 2017, 36, 407-421.	8.9	107
30	Automatic segmentation of up to ten layer boundaries in SD-OCT images of the mouse retina with and without missing layers due to pathology. Biomedical Optics Express, 2014, 5, 348.	2.9	104
31	Robust automatic segmentation of corneal layer boundaries in SDOCT images using graph theory and dynamic programming. Biomedical Optics Express, 2011, 2, 1524.	2.9	101
32	Quantitative Comparison of Drusen Segmented on SD-OCT versus Drusen Delineated on Color Fundus Photographs. , 2010, 51, 4875.		99
33	Spectral-Domain Optical Coherence Tomographic Assessment of Severity of Cystoid Macular Edema in Retinopathy of Prematurity. JAMA Ophthalmology, 2012, 130, 569-78.	2.4	98
34	Characterization of the Choroid-Scleral Junction and Suprachoroidal Layer in Healthy Individuals on Enhanced-Depth Imaging Optical Coherence Tomography. JAMA Ophthalmology, 2014, 132, 174.	2.5	93
35	Drusen Volume and Retinal Pigment Epithelium Abnormal Thinning Volume Predict 2-Year Progression of Age-Related Macular Degeneration. Ophthalmology, 2016, 123, 39-50.e1.	5.2	92
36	Fast and robust active neuron segmentation in two-photon calcium imaging using spatiotemporal deep learning. Proceedings of the National Academy of Sciences of the United States of America, 2019, 116, 8554-8563.	7.1	91

#	Article	IF	CITATIONS
37	Visualization of conventional outflow tissue responses to netarsudil in living mouse eyes. European Journal of Pharmacology, 2016, 787, 20-31.	3.5	89
38	Evaluation of inner retinal layers as biomarkers in mild cognitive impairment to moderate Alzheimer's disease. PLoS ONE, 2018, 13, e0192646.	2.5	88
39	Effect of Anti–Vascular Endothelial Growth Factor Therapy on Choroidal Thickness in Diabetic Macular Edema. American Journal of Ophthalmology, 2014, 158, 745-751.e2.	3.3	87
40	Visualization of Real-Time Intraoperative Maneuvers with a Microscope-Mounted Spectral Domain Optical Coherence Tomography System. Retina, 2013, 33, 232-236.	1.7	83
41	Spatial Correlation between Hyperpigmentary Changes on Color Fundus Photography and Hyperreflective Foci on SDOCT in Intermediate AMD. , 2012, 53, 4626.		80
42	Relationship of Central Choroidal Thickness With Age-Related Macular Degeneration Status. American Journal of Ophthalmology, 2015, 159, 617-626.e2.	3.3	77
43	Optical Coherence Tomography Predictors of Risk for Progression to Non-Neovascular Atrophic Age-Related Macular Degeneration. Ophthalmology, 2017, 124, 1764-1777.	5.2	77
44	Efficient Fourier-Wavelet Super-Resolution. IEEE Transactions on Image Processing, 2010, 19, 2669-2681.	9.8	76
45	Automatic cone photoreceptor segmentation using graph theory and dynamic programming. Biomedical Optics Express, 2013, 4, 924.	2.9	75
46	Pilocarpine-Induced Dilation of Schlemm's Canal and Prevention of Lumen Collapse at Elevated Intraocular Pressures in Living Mice Visualized by OCT. , 2014, 55, 3737.		74
47	Analysis of Pars Plana Vitrectomy for Optic Pit–Related Maculopathy With Intraoperative Optical Coherence Tomography. JAMA Ophthalmology, 2011, 129, 1483.	2.4	73
48	Proteomic Profiling of a Layered Tissue Reveals Unique Glycolytic Specializations of Photoreceptor Cells. Molecular and Cellular Proteomics, 2011, 10, M110.002469.	3.8	72
49	Anatomy and spatial organization of Müller glia in mouse retina. Journal of Comparative Neurology, 2017, 525, 1759-1777.	1.6	71
50	Choroid Development and Feasibility of Choroidal Imaging in the Preterm and Term Infants Utilizing SD-OCT. , 2013, 54, 4140.		69
51	Optical Coherence Tomography Reflective Drusen Substructures Predict Progression to Geographic Atrophy in Age-related Macular Degeneration. Ophthalmology, 2016, 123, 2554-2570.	5.2	69
52	Fully Automatic Segmentation of Fluorescein Leakage in Subjects With Diabetic Macular Edema. Investigative Ophthalmology and Visual Science, 2015, 56, 1482-1492.	3.3	68
53	Handheld simultaneous scanning laser ophthalmoscopy and optical coherence tomography system. Biomedical Optics Express, 2013, 4, 2307.	2.9	66
54	In vivo measurement of trabecular meshwork stiffness in a corticosteroid-induced ocular hypertensive mouse model. Proceedings of the National Academy of Sciences of the United States of America, 2019, 116, 1714-1722.	7.1	66

#	Article	IF	CITATIONS
55	Automatic segmentation of closed-contour features in ophthalmic images using graph theory and dynamic programming. Biomedical Optics Express, 2012, 3, 1127.	2.9	65
56	Open source software for automatic detection of cone photoreceptors in adaptive optics ophthalmoscopy using convolutional neural networks. Scientific Reports, 2017, 7, 6620.	3.3	65
57	Correction of Ocular Shape in Retinal Optical Coherence Tomography and Effect on Current Clinical Measures. American Journal of Ophthalmology, 2013, 156, 304-311.	3.3	58
58	Fully Automatic Software for Retinal Thickness in Eyes With Diabetic Macular Edema From Images Acquired by Cirrus and Spectralis Systems. , 2013, 54, 7595.		58
59	Automatic detection of cone photoreceptors in split detector adaptive optics scanning light ophthalmoscope images. Biomedical Optics Express, 2016, 7, 2036.	2.9	55
60	Deep learning-based single-shot prediction of differential effects of anti-VEGF treatment in patients with diabetic macular edema. Biomedical Optics Express, 2020, 11, 1139.	2.9	53
61	Retinal nerve fiber layer thickness in amnestic mild cognitive impairment: Case ontrol study and metaâ€∎nalysis. Alzheimer's and Dementia: Diagnosis, Assessment and Disease Monitoring, 2016, 4, 85-93.	2.4	51
62	Robust shift and add approach to superresolution. , 2003, , .		50
63	Optical coherence refraction tomography. Nature Photonics, 2019, 13, 794-802.	31.4	50
64	Multimodal Characterization of Proliferative Diabetic Retinopathy Reveals Alterations in Outer Retinal Function and Structure. Ophthalmology, 2015, 122, 957-967.	5.2	49
65	Deep longitudinal transfer learning-based automatic segmentation of photoreceptor ellipsoid zone defects on optical coherence tomography images of macular telangiectasia type 2. Biomedical Optics Express, 2018, 9, 2681.	2.9	48
66	Tree Topology Estimation. IEEE Transactions on Pattern Analysis and Machine Intelligence, 2015, 37, 1688-1701.	13.9	47
67	Longitudinal Associations Between Microstructural Changes and Microperimetry in the Early Stages of Age-Related Macular Degeneration. , 2016, 57, 3714.		46
68	Repeatability of Choroidal Thickness Measurements on Enhanced Depth Imaging Optical Coherence Tomography Using Different Posterior Boundaries. American Journal of Ophthalmology, 2016, 169, 104-112.	3.3	43
69	Relating Retinal Morphology and Function in Aging and Early to Intermediate Age-related Macular Degeneration Subjects. American Journal of Ophthalmology, 2016, 165, 65-77.	3.3	43
70	Subfoveal Fluid in Healthy Full-term Newborns Observed by Handheld Spectral-Domain Optical Coherence Tomography. American Journal of Ophthalmology, 2012, 153, 167-175.e3.	3.3	42
71	Choroidal Changes After Suprachoroidal Injection of Triamcinolone Acetonide in Eyes With Macular Edema Secondary to Retinal Vein Occlusion. American Journal of Ophthalmology, 2018, 186, 144-151.	3.3	42
72	Deep learning based detection of cone photoreceptors with multimodal adaptive optics scanning light ophthalmoscope images of achromatopsia. Biomedical Optics Express, 2018, 9, 3740.	2.9	41

#	Article	IF	CITATIONS
73	Effect of Uveal Melanocytes on Choroidal Morphology in Rhesus Macaques and Humans on Enhanced-Depth Imaging Optical Coherence Tomography. , 2016, 57, 5764.		40
74	In vivo cellular-resolution retinal imaging in infants and children using an ultracompact handheld probe. Nature Photonics, 2016, 10, 580-584.	31.4	40
75	Wide-field retinal optical coherence tomography with wavefront sensorless adaptive optics for enhanced imaging of targeted regions. Biomedical Optics Express, 2017, 8, 16.	2.9	40
76	Video-to-Video Dynamic Super-Resolution for Grayscale and Color Sequences. Eurasip Journal on Advances in Signal Processing, 2006, 2006, 1.	1.7	39
77	Optical Coherence Tomography Accurately Measures Corneal Power Change from Laser Refractive Surgery. Ophthalmology, 2015, 122, 677-686.	5.2	39
78	Posterior Eye Shape Measurement With Retinal OCT Compared to MRI. , 2016, 57, OCT196.		39
79	In Vivo Multimodal Imaging of Drusenoid Lesions in Rhesus Macaques. Scientific Reports, 2017, 7, 15013.	3.3	38
80	Exploratory Dijkstra forest based automatic vessel segmentation: applications in video indirect ophthalmoscopy (VIO). Biomedical Optics Express, 2012, 3, 327.	2.9	37
81	The Effects of Diabetic Retinopathy and Pan-Retinal Photocoagulation on Photoreceptor Cell Function as Assessed by Dark Adaptometry. , 2016, 57, 208.		36
82	Real-time corneal segmentation and 3D needle tracking in intrasurgical OCT. Biomedical Optics Express, 2018, 9, 2716.	2.9	36
83	Statistical Models of Signal and Noise and Fundamental Limits of Segmentation Accuracy in Retinal Optical Coherence Tomography. IEEE Transactions on Medical Imaging, 2018, 37, 1978-1988.	8.9	36
84	Robust Kernel Regression for Restoration and Reconstruction of Images from Sparse Noisy Data. , 2006, , .		33
85	Intrasurgical Human Retinal Imaging With Manual Instrument Tracking Using a Microscope-Integrated Spectral-Domain Optical Coherence Tomography Device. Translational Vision Science and Technology, 2015, 4, 1.	2.2	33
86	Physical Factors Affecting Outflow Facility Measurements in Mice. , 2015, 56, 8331.		33
87	Impact of Microscope-Integrated OCT on Ophthalmology Resident Performance of Anterior Segment Surgical Maneuvers in Model Eyes. , 2016, 57, OCT146.		32
88	Needle Depth and Big-Bubble Success in Deep Anterior Lamellar Keratoplasty. Cornea, 2016, 35, 1471-1477.	1.7	32
89	Macular sub-layer thinning and association with pulmonary function tests in Amyotrophic Lateral Sclerosis. Scientific Reports, 2016, 6, 29187.	3.3	32
90	Anti-fibrotic activity of a rho-kinase inhibitor restores outflow function and intraocular pressure homeostasis. ELife, 2021, 10, .	6.0	32

#	Article	IF	CITATIONS
91	Enhanced video indirect ophthalmoscopy (VIO) via robust mosaicing. Biomedical Optics Express, 2011, 2, 2871.	2.9	31
92	Optimization of confocal scanning laser ophthalmoscope design. Journal of Biomedical Optics, 2013, 18, 076015.	2.6	31
93	Length-adaptive graph search for automatic segmentation of pathological features in optical coherence tomography images. Journal of Biomedical Optics, 2016, 21, 076015.	2.6	31
94	Comparison of chorioretinal layers in rhesus macaques using spectral-domain optical coherence tomography and high-resolution histological sections. Experimental Eye Research, 2018, 168, 69-76.	2.6	31
95	Evaluation of Contrast Agents for Enhanced Visualization in Optical Coherence Tomography. , 2010, 51, 6614.		30
96	Interlaced spectrally encoded confocal scanning laser ophthalmoscopy and spectral domain optical coherence tomography. Biomedical Optics Express, 2010, 1, 431.	2.9	30
97	Enhanced visualization of peripheral retinal vasculature with wavefront sensorless adaptive optics optical coherence tomography angiography in diabetic patients. Optics Letters, 2017, 42, 17.	3.3	30
98	RAC-CNN: multimodal deep learning based automatic detection and classification of rod and cone photoreceptors in adaptive optics scanning light ophthalmoscope images. Biomedical Optics Express, 2019, 10, 3815.	2.9	30
99	Correlation Between Macular Integrity Assessment and Optical Coherence Tomography Imaging of Ellipsoid Zone in Macular Telangiectasia Type 2. , 2017, 58, BIO291.		29
100	Image Inversion Spectral-Domain Optical Coherence Tomography Optimizes Choroidal Thickness and Detail through Improved Contrast. , 2012, 53, 1874.		28
101	A Quantitative Approach to Predict Differential Effects of Anti-VEGF Treatment on Diffuse and Focal Leakage in Patients with Diabetic Macular Edema: A Pilot Study. Translational Vision Science and Technology, 2017, 6, 7.	2.2	28
102	Statistical detection and imaging of objects hidden in turbid media using ballistic photons. Applied Optics, 2007, 46, 5805.	2.1	27
103	Fast detection and segmentation of drusen in retinal optical coherence tomography images. Proceedings of SPIE, 2008, , .	0.8	27
104	True color scanning laser ophthalmoscopy and optical coherence tomography handheld probe. Biomedical Optics Express, 2014, 5, 3204.	2.9	27
105	Beyond Performance Metrics. Ophthalmology, 2020, 127, 793-801.	5.2	27
106	Long-term Evolution and Remodeling of Soft Drusen in Rhesus Macaques. , 2020, 61, 32.		27
107	Segmentation of neurons from fluorescence calcium recordings beyond real time. Nature Machine Intelligence, 2021, 3, 590-600.	16.0	27
108	Lateral and axial measurement differences between spectral-domain optical coherence tomography systems. Journal of Biomedical Optics, 2014, 19, 016014.	2.6	26

#	Article	IF	CITATIONS
109	3-D Adaptive Sparsity Based Image Compression With Applications to Optical Coherence Tomography. IEEE Transactions on Medical Imaging, 2015, 34, 1306-1320.	8.9	26
110	Assessment of Retinal Nerve Fiber Layer Thickness in Healthy, Full-Term Neonates. American Journal of Ophthalmology, 2015, 159, 803-811.e2.	3.3	26
111	Handheld adaptive optics scanning laser ophthalmoscope. Optica, 2018, 5, 1027.	9.3	26
112	Distributed scanning volumetric SDOCT for motion corrected corneal biometry. Biomedical Optics Express, 2012, 3, 2050.	2.9	25
113	Hybrid light-sheet and light-field microscope for high resolution and large volume neuroimaging. Biomedical Optics Express, 2019, 10, 6595.	2.9	25
114	Novel Image-Based Analysis for Reduction of Clinician-Dependent Variability in Measurement of the Corneal Ulcer Size. Cornea, 2018, 37, 331-339.	1.7	23
115	Ocular amyloid imaging at the crossroad of Alzheimer's disease and age-related macular degeneration: implications for diagnosis and therapy. Journal of Neurology, 2019, 266, 1566-1577.	3.6	23
116	Computational modeling of retinal hypoxia and photoreceptor degeneration in patients with age-related macular degeneration. PLoS ONE, 2019, 14, e0216215.	2.5	22
117	MimickNet, Mimicking Clinical Image Post- Processing Under Black-Box Constraints. IEEE Transactions on Medical Imaging, 2020, 39, 2277-2286.	8.9	22
118	BiconNet: An edge-preserved connectivity-based approach for salient object detection. Pattern Recognition, 2022, 121, 108231.	8.1	22
119	Baseline Visual Field Findings in the RUSH2A Study: Associated Factors and Correlation With Other Measures of Disease Severity. American Journal of Ophthalmology, 2020, 219, 87-100.	3.3	22
120	Semiautomatic Segmentation of Rim Area Focal Hyperautofluorescence Predicts Progression of Geographic Atrophy Due to Dry Age-Related Macular Degeneration. , 2016, 57, 2283.		21
121	INTRAOPERATIVE SPECTRAL DOMAIN OPTICAL COHERENCE TOMOGRAPHY IMAGING AFTER INTERNAL LIMITING MEMBRANE PEELING IN IDIOPATHIC EPIRETINAL MEMBRANE WITH CONNECTING STRANDS. Retina, 2015, 35, 1622-1630.	1.7	20
122	Vascular Response to Sildenafil Citrate in Aging and Age-Related Macular Degeneration. Scientific Reports, 2019, 9, 5049.	3.3	20
123	Super-resolution retinal imaging using optically reassigned scanning laser ophthalmoscopy. Nature Photonics, 2019, 13, 257-262.	31.4	20
124	Integral role for lysyl oxidaseâ€likeâ€1 in conventional outflow tissue function and behavior. FASEB Journal, 2020, 34, 10762-10777.	0.5	20
125	Multiframe demosaicing and super-resolution from undersampled color images. , 2004, 5299, 222.		19
126	Coherence revival multiplexed, buffered swept source optical coherence tomography: 400  kHz imaging with a 100  kHz source. Optics Letters, 2014, 39, 3740.	3.3	19

#	Article	IF	CITATIONS
127	Weakly supervised individual ganglion cell segmentation from adaptive optics OCT images for glaucomatous damage assessment. Optica, 2021, 8, 642.	9.3	19
128	Disease progression in iridocorneal angle tissues of BMP2-induced ocular hypertensive mice with optical coherence tomography. Molecular Vision, 2014, 20, 1695-709.	1.1	18
129	Segmentation guided registration of wide field-of-view retinal optical coherence tomography volumes. Biomedical Optics Express, 2016, 7, 4827.	2.9	17
130	Validation of Macular Choroidal Thickness Measurements from Automated SD-OCT Image Segmentation. Optometry and Vision Science, 2016, 93, 1387-1398.	1.2	17
131	Distribution of OCT Features within Areas of Macular Atrophy or Scar after 2 Years of Anti-VEGF Treatment for Neovascular AMD in CATT. Ophthalmology Retina, 2019, 3, 316-325.	2.4	17
132	Open-Source Automatic Segmentation of Ocular Structures and Biomarkers of Microbial Keratitis on Slit-Lamp Photography Images Using Deep Learning. IEEE Journal of Biomedical and Health Informatics, 2021, 25, 88-99.	6.3	17
133	Macular Fluid Reduces Reproducibility of Choroidal Thickness Measurements on Enhanced Depth Optical Coherence Tomography. American Journal of Ophthalmology, 2017, 184, 108-114.	3.3	16
134	Multimodal Coherent Imaging of Retinal Biomarkers of Alzheimer's Disease in a Mouse Model. Scientific Reports, 2020, 10, 7912.	3.3	16
135	Corneal biometry from volumetric SDOCT and comparison with existing clinical modalities. Biomedical Optics Express, 2012, 3, 1279.	2.9	15
136	Retinal Atrophy in Eyes With Resolved Papilledema Detected by Optical Coherence Tomography. Journal of Neuro-Ophthalmology, 2015, 35, 122-126.	0.8	15
137	Assessing Ganglion Cell Layer Topography in Human Albinism Using Optical Coherence Tomography. , 2020, 61, 36.		15
138	Unified k-space theory of optical coherence tomography. Advances in Optics and Photonics, 2021, 13, 462.	25.5	15
139	Macular Findings in Healthy Full-term Hispanic Newborns Observed by Hand-held Spectral-Domain Optical Coherence Tomography. Ophthalmic Surgery Lasers and Imaging Retina, 2013, 44, 448-454.	0.7	15
140	Analyzing spatial correlations in tissue using angle-resolved low coherence interferometry measurements guided by co-located optical coherence tomography. Biomedical Optics Express, 2016, 7, 1400.	2.9	14
141	Prediction of lupus nephritis in patients with systemic lupus erythematosus using artificial neural networks. Lupus, 2002, 11, 485-492.	1.6	13
142	<title>Dynamic demosaicing and color superresolution of video sequences</title> ., 2004, , .		13
143	Power Trace: An Efficient Method for Extracting the Power Dissipation Profile in an IC Chip From Its Temperature Map. IEEE Transactions on Components and Packaging Technologies, 2009, 32, 309-316.	1.3	13
144	Compressed wavefront sensing. Optics Letters, 2014, 39, 1189.	3.3	13

#	Article	IF	CITATIONS
145	Higher order bilateral filters and their properties. , 2007, , .		11
146	Retinal cavitations in macular telangiectasia type 2 (MacTel): longitudinal structure–function correlations. British Journal of Ophthalmology, 2021, 105, 109-112.	3.9	11
147	Connectivity-based deep learning approach for segmentation of the epithelium in in vivo human esophageal OCT images. Biomedical Optics Express, 2021, 12, 6326.	2.9	11
148	Platform-Independent Cirrus and Spectralis Thickness Measurements in Eyes with Diabetic Macular Edema Using Fully Automated Software. Translational Vision Science and Technology, 2017, 6, 9.	2.2	10
149	Linking OCT, Angiographic, and Photographic Lesion Components in Neovascular Age-Related Macular Degeneration. Ophthalmology Retina, 2018, 2, 481-493.	2.4	10
150	A practical approach to superresolution. , 2006, 6077, 24.		9
151	Demonstration of anatomical development of the human macula within the first 5Âyears of life using handheld OCT. International Ophthalmology, 2019, 39, 1533-1542.	1.4	9
152	COMPARISON OF SINGLE DRUSEN SIZE ON COLOR FUNDUS PHOTOGRAPHY AND SPECTRAL-DOMAIN OPTICAL COHERENCE TOMOGRAPHY. Retina, 2021, 41, 1715-1722.	1.7	9
153	Spectroscopic optical coherence refraction tomography. Optics Letters, 2020, 45, 2091.	3.3	9
154	Effects of aging and environmental tobacco smoke exposure on ocular and plasma circulatory microRNAs in the Rhesus macaque. Molecular Vision, 2018, 24, 633-646.	1.1	9
155	Deep learning-based classification and segmentation of retinal cavitations on optical coherence tomography images of macular telangiectasia type 2. British Journal of Ophthalmology, 2022, 106, 396-402.	3.9	8
156	Local Anatomic Precursors to New-Onset Geographic Atrophy in Age-Related Macular Degeneration as Defined on OCT. Ophthalmology Retina, 2021, 5, 396-408.	2.4	8
157	Open-source, machine and deep learning-based automated algorithm for gestational age estimation through smartphone lens imaging. Biomedical Optics Express, 2018, 9, 6038.	2.9	8
158	Computational 3D microscopy with optical coherence refraction tomography. Optica, 0, , .	9.3	8
159	Efficient Registration of Aliased X-Ray Images. Conference Record of the Asilomar Conference on Signals, Systems and Computers, 2007, , .	0.0	7
160	Characterization of Long Working Distance Optical Coherence Tomography for Imaging of Pediatric Retinal Pathology. Translational Vision Science and Technology, 2017, 6, 12.	2.2	7
161	Quantitative Fundus Autofluorescence in Rhesus Macaques in Aging and Age-Related Drusen. , 2020, 61, 16.		7
162	Generative adversarial networks to predict treatment response for neovascular age-related macular degeneration: interesting, but is it useful?. British Journal of Ophthalmology, 2020, 104, 1629-1630.	3.9	6

#	Article	IF	CITATIONS
163	Learning Partial Differential Equations From Data Using Neural Networks. , 2020, , .		6
164	Lightweight Learning-Based Automatic Segmentation of Subretinal Blebs on Microscope-Integrated Optical Coherence Tomography Images. American Journal of Ophthalmology, 2021, 221, 154-168.	3.3	6
165	Multimodal handheld adaptive optics scanning laser ophthalmoscope. Optics Letters, 2020, 45, 4940.	3.3	6
166	Open-source deep learning-based automatic segmentation of mouse Schlemm's canal in optical coherence tomography images. Experimental Eye Research, 2022, 214, 108844.	2.6	6
167	Machine Learning OCT Predictors of Progression from Intermediate Age-Related Macular Degeneration to Geographic Atrophy and Vision Loss. Ophthalmology Science, 2022, 2, 100160.	2.5	6
168	Extraction of Power Dissipation Profile in an IC Chip from Temperature Map. IEEE Semiconductor Thermal Measurement and Management Symposium, 2007, , .	0.0	5
169	Estimation of Gestational Age via Image Analysis of Anterior Lens Capsule Vascularity in Preterm Infants: A Pilot Study. Frontiers in Pediatrics, 2019, 7, 43.	1.9	5
170	VALIDATION OF A DEEP LEARNING-BASED ALGORITHM FOR SEGMENTATION OF THE ELLIPSOID ZONE ON OPTICAL COHERENCE TOMOGRAPHY IMAGES OF AN USH2A-RELATED RETINAL DEGENERATION CLINICAL TRIAL. Retina, 2022, 42, 1347-1355.	1.7	5
171	Efficient restoration and enhancement of super-resolved X-ray images. , 2008, , .		4
172	Generalized pseudo-polar Fourier grids and applications in registering ophthalmic optical coherence tomography images. , 2009, , .		4
173	Retinal imaging in human autopsy eyes using a custom optical coherence tomography periscope. Biomedical Optics Express, 2017, 8, 4152.	2.9	4
174	Information-Theoretic Approach and Fundamental Limits of Resolving Two Closely Timed Neuronal Spikes in Mouse Brain Calcium Imaging. IEEE Transactions on Biomedical Engineering, 2018, 65, 2428-2439.	4.2	4
175	Measurement Reliability for Keratitis Morphology. Cornea, 2020, 39, 1503-1509.	1.7	4
176	Mesoscopic photogrammetry with an unstabilized phone camera. , 2021, , .		4
177	Identifying Latent Stochastic Differential Equations. IEEE Transactions on Signal Processing, 2022, 70, 89-104.	5.3	4
178	Understanding RPE Lipofuscin. , 2016, 57, 6766.		3
179	MimickNet, Matching Clinical Post-Processing Under Realistic Black-Box Constraints. , 2019, , .		3
180	Microscope-Integrated OCT-Guided Volumetric Measurements of Subretinal Blebs Created by a Suprachoroidal Approach. Translational Vision Science and Technology, 2021, 10, 24.	2.2	3

#	Article	IF	CITATIONS
181	Open-Source Automatic Biomarker Measurement on Slit-Lamp Photography to Estimate Visual Acuity in Microbial Keratitis. Translational Vision Science and Technology, 2021, 10, 2.	2.2	3
182	Novel approaches to high-speed multi-view imaging approaching 4pi steradians using conic section mirrors: theoretical and practical considerations. Journal of the Optical Society of America A: Optics and Image Science, and Vision, 0, , .	1.5	3
183	Integrated Visualization Highlighting Retinal Changes in Retinopathy of Prematurity From 3-Dimensional Optical Coherence Tomography Data. JAMA Ophthalmology, 2022, 140, 725.	2.5	3
184	Regularized Kernel Regression for Image Deblurring. , 2006, , .		2
185	Treated PDR Reveals Age-Appropriate Vision Deterioration But Distorted Retinal Organization. Translational Vision Science and Technology, 2020, 9, 3.	2.2	2
186	Intraoperative Retinal Changes May Predict Surgical Outcomes After Epiretinal Membrane Peeling. Translational Vision Science and Technology, 2021, 10, 36.	2.2	2
187	Using an Image Fusion Methodology to Improve Efficiency and Traceability of Posterior Pole Vessel Analysis by ROPtool. Open Ophthalmology Journal, 2017, 11, 143-151.	0.2	2
188	Anatomy and spatial organization of Müller glia in mouse retina. Journal of Comparative Neurology, 2017, 525, spc1-spc1.	1.6	1
189	Reply. American Journal of Ophthalmology, 2018, 189, 178.	3.3	1
190	Applications of Spectral-Domain OCT in AMD. , 2009, , 15-34.		1
191	Fully automatic quantification of individual ganglion cells from AO-OCT volumes via weakly supervised learning. , 2020, , .		1
192	Incoherent 3D k-space synthesis with volumetric optical coherence refraction tomography. , 2021, , .		1
193	Multi-Scale Statistical Detection and Ballistic Imaging Through Turbid Media. , 2007, , .		0
194	Segmentation of ophthalmic optical coherence tomography images using graph cuts. , 2010, , .		0
195	Distributed Scan SDOCT Improves Post Refractive Surgery Corneal Biometry. , 2012, , .		0
196	Ultra-compact switchable SLO/OCT handheld probe design. , 2015, , .		0
197	Reply. Ophthalmology, 2016, 123, e6-e7.	5.2	0
198	57084 Combining artificial intelligence and robotics: a novel fully automated optical coherence tomography-based approach for eye disease screening. Journal of Clinical and Translational Science, 2021, 5, 122-122.	0.6	0

#	Article	IF	CITATIONS
199	Resolution enhancement and speckle reduction in coherence imaging: a k-space model of optical coherence refraction tomography (OCRT). , 2020, , .		о
200	Wavefront sensorless multimodal handheld adaptive optics scanning laser ophthalmoscope for in vivo imaging of human retinal cones. , 2020, , .		0
201	Editorial from the New Editor-in-Chief and the New Deputy Editor. Biomedical Optics Express, 2022, 13, 980.	2.9	0
202	Fast and accurate neuron segmentation and unmixing based on shallow U-Net. , 2022, , .		0